

Magnetized accretion disks around Kerr black holes with scalar hair - I. Constant angular momentum

Sergio Gimeno-Soler,¹ José A. Font,^{1, 2} Carlos Herdeiro,³ and Eugen Radu³

¹*Departamento de Astronomía y Astrofísica, Universitat de València,
Dr. Moliner 50, 46100, Burjassot (València), Spain*

²*Observatori Astronòmic, Universitat de València,
C/ Catedrático José Beltrán 2, 46980, Paterna (València), Spain*

³*Departamento de Física da Universidade de Aveiro and CIDMA, Campus de Santiago, 3810-183 Aveiro, Portugal*
(Dated: June 1, 2018)

We present a method to build magnetized constant angular momentum disks around Kerr black holes with scalar hair (KBHsSH).

PACS numbers: 95.30.Sf, 04.70.Bw, 04.40.Nr, 04.25.dg

I. INTRODUCTION

II.

III. FRAMEWORK

We use the stationary and axisymmetric metric ansatz provided by[1]

$$ds^2 = e^{2F_1} \left(\frac{dr^2}{N} + r^2 d\theta^2 \right) + e^{2F_2} r^2 \sin^2 \theta (d\phi - W dt)^2 - e^{2F_0} N dt^2, \quad (1)$$

with $N = 1 - r_H/r$, where r_H is the radius of the event horizon of the BH and W, F_1, F_2, F_0 are functions of r and θ .

This metric is a solution to the Einstein-Klein-Gordon field equations $R_{ab} - \frac{1}{2}Rg_{ab} = 8\pi G(T_{SF})_{ab}$ with

$$(T_{SF})_{ab} = \partial_a \Psi^* \partial_b \Psi + \partial_b \Psi^* \partial_a \Psi - g_{ab} \left(\frac{1}{2} g^{cd} (\partial_c \Psi^* \partial_d \Psi + \partial_d \Psi^* \partial_c \Psi) + \mu^2 \Psi^* \Psi \right), \quad (2)$$

where Ψ is a complex Klein-Gordon field such as $\Psi = \phi(r, \theta) e^{im\phi} - wt$ where w is the scalar field frequency and m is the azimuthal harmonic index.

A. Distribution of angular momentum and equations of motion

We introduce the specific angular momentum l and the angular velocity Ω employing the standard definitions,

$$l = -\frac{u_\phi}{u_t}, \quad \Omega = \frac{u^\phi}{u^t}, \quad (3)$$

where u^μ is the fluid four-velocity. The relationship between l and Ω is given by the equations

$$l = -\frac{\Omega g_{\phi\phi} + g_{t\phi}}{\Omega g_{t\phi} + g_{tt}}, \quad \Omega = -\frac{l g_{tt} + g_{t\phi}}{l g_{t\phi} + g_{\phi\phi}}, \quad (4)$$

where we are assuming circular motion, i.e. the four-velocity can be written as

$$u^\mu = (u^t, 0, 0, u^\phi). \quad (5)$$

We consider a constant angular momentum distribution $l(r, \theta) = \text{cte.}$. The specific value of the angular momentum is computed as the minimum of the following equation

$$l_b^\pm(r, \theta) = \frac{g_{t\phi} \pm \left(\sqrt{g_{t\phi}^2 - g_{tt}g_{t\phi}} \right) \sqrt{1 + g_{tt}}}{-g_{tt}} \quad (6)$$

where the plus sign is for prograde orbits and the minus is for retrograde orbits. This expression is given by [2] for Kerr BHs, but it is valid for any stationary, axisymmetric spacetimes. For prograde motion, the function has a minimum outside the event horizon. The location of said minimum corresponds with the marginally bound orbit r_{mb} , and the angular momentum corresponds to the keplerian angular momentum l_{mb} at that point. We show the proof of this statement at appendix C. This choice of angular momentum distribution is motivated by its simplicity (for a first study of thick tori around KBHsSH) and for allowing the presence of a cusp (to allow matter accretion onto the black hole) and a centre.

B. Magnetized disks

We use the procedure described by [3], where we write the equations of ideal general relativistic MHD as the following conservation laws, $\nabla_\mu T^{\mu\nu} = 0$, $\nabla_\mu {}^*F^{\mu\nu} = 0$, and $\nabla_\mu (\rho u^\mu) = 0$, where ∇_μ is the covariant derivative and

$$T^{\mu\nu} = (\rho h + b^2) u^\mu u^\nu + \left(p + \frac{1}{2} b^2 \right) g^{\mu\nu} - b^\mu b^\nu, \quad (7)$$

is the energy-momentum tensor of a magnetised perfect fluid, h , ρ p being the fluid specific enthalpy, density and fluid pressure, respectively. Moreover, ${}^*F^{\mu\nu} = b^\mu u^\nu - b^\nu u^\mu$ is the (dual of the) Faraday tensor relative

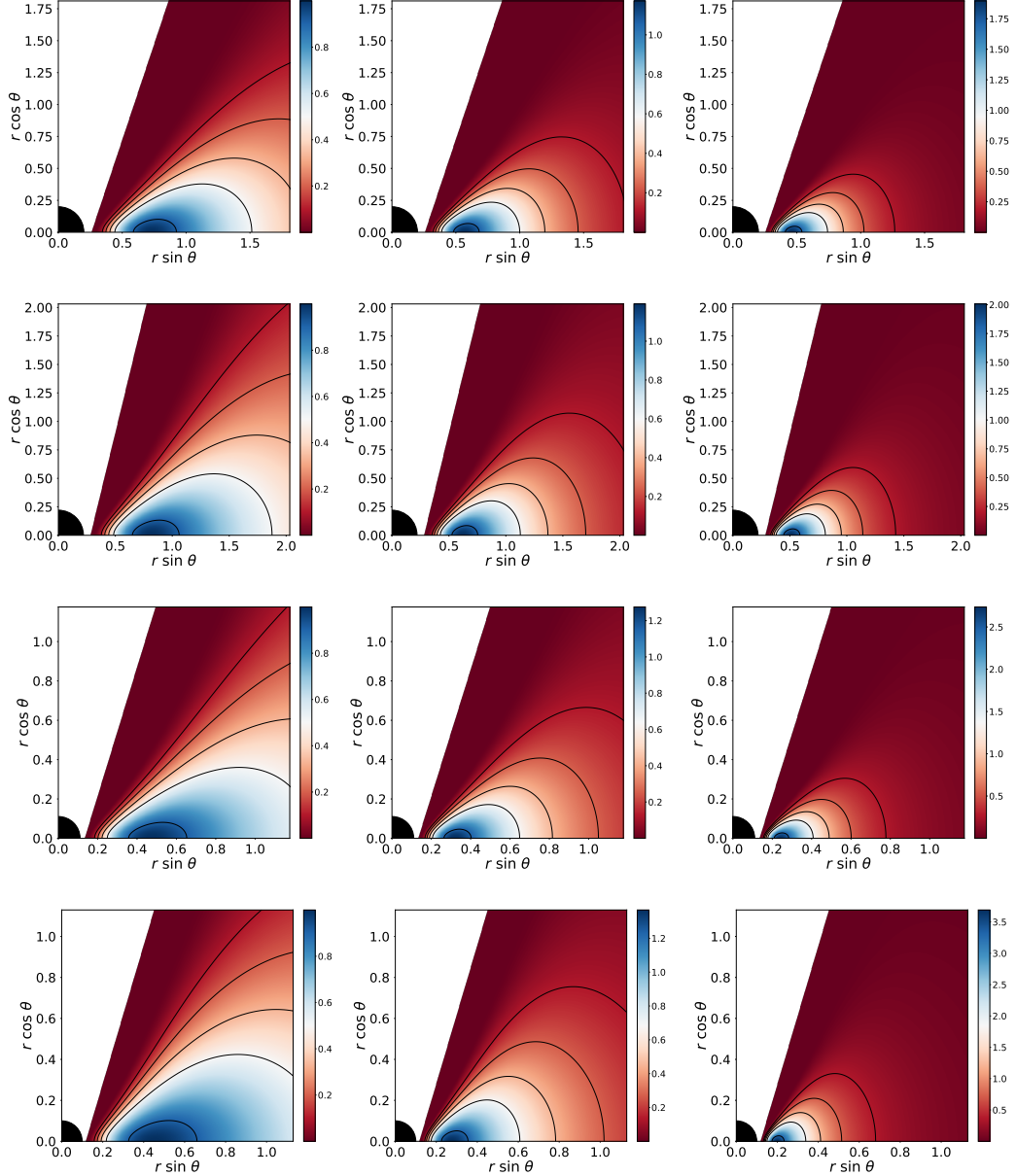


FIG. 1. Rest-mass density distribution. From top to bottom the rows correspond to the different models for the KBHsSH (I, II, III and IV). From left to right the columns correspond to different values of the magnetization parameter, namely non-magnetized ($\beta_{mc} = 10^{10}$), mildly magnetized ($\beta_{mc} = 1$) and strongly magnetized ($\beta_{mc} = 10^{-10}$)

to an observer with four-velocity u^μ , and b^μ is the magnetic field in that frame, with $b^2 = b^\mu b_\mu$. Assuming the magnetic field is purely azimuthal, i.e. $b^r = b^\theta = 0$, and taking into account that the flow is stationary and axisymmetric, the conservation of the current density and of the Faraday tensor follow. Contracting the divergence of Eq. (7) with the projection tensor $h^\alpha_\beta = \delta^\alpha_\beta + u^\alpha u_\beta$, we arrive at

$$(\rho h + b^2)u_\nu \partial_i u^\nu + \partial_i \left(p + \frac{b^2}{2} \right) - b_\nu \partial_i b^\nu = 0, \quad (8)$$

where $i = r, \theta$. Then, we rewrite this equation in terms

of the specific angular momentum l and of the angular velocity Ω , to obtain

$$\partial_i (\ln u_t) - \frac{\Omega \partial_i l}{1 - l\Omega} + \frac{\partial_i p}{w} + \frac{\partial_i (\mathcal{L}b^2)}{2\mathcal{L}w} = 0, \quad (9)$$

where $\mathcal{L} = g_{t\phi}^2 - g_{tt}g_{\phi\phi}$.

$$\mathcal{L} = g_{t\phi}^2 - g_{tt}g_{\phi\phi}. \quad (10)$$

To integrate Eq. (9) we first assume a polytropic equation

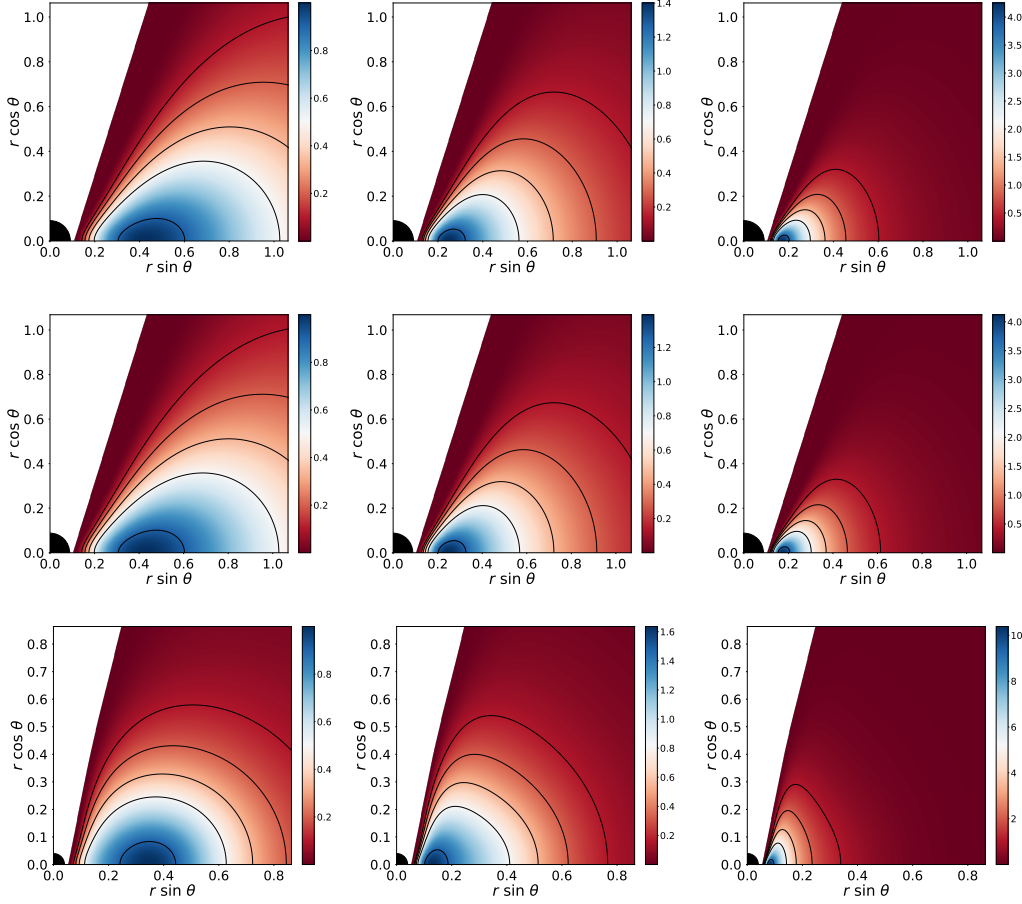


FIG. 2. Rest-mass density distribution. From top to bottom the rows correspond to the different models for the KBHsSH (V, VI and VII). From left to right the columns correspond to different values of the magnetization parameter, namely non-magnetized ($\beta_{mc} = 10^{10}$), mildly magnetized ($\beta_{mc} = 1$) and strongly magnetized ($\beta_{mc} = 10^{-10}$)

of state of the form

$$p = K\rho^\Gamma, \quad (11)$$

with K and Γ constants. Then, we define the magnetic pressure as $p_m = b^2/2$, and introduce the definitions $\tilde{p}_m = \mathcal{L}p_m$ and $\tilde{w} = \mathcal{L}w$, in order to write an analogue equation to Eq. (11) for \tilde{p}_m [4]

$$\tilde{p}_m = M\tilde{w}^q, \quad (12)$$

or, in terms of the magnetic pressure p_m

$$p_m = M\mathcal{L}^{q-1}w^q, \quad (13)$$

where $w = \rho h$ is the fluid enthalpy density, and M and q are constants. If we define the potential as $W \equiv \ln|u_t|$, then we can integrate the equation (9) as

$$W - W_{in} + \ln\left(1 + \frac{\Gamma K}{\Gamma + 1}\rho^{\gamma-1}\right) + \frac{q}{q-1}M(\mathcal{L}w)^{q-1} = 0, \quad (14)$$

where W_{in} is the potential at the inner edge of the disk.

We also write the expressions of the total energy density for the torus ρ_T :

$$\rho_T = -T_t^t + T_i^i = \frac{\rho h(g_{\phi\phi} - g_{tt}l^2)}{g_{\phi\phi} + 2g_{t\phi}l + g_{tt}l^2} + 2(p + p_m), \quad (15)$$

and the total energy density for the scalar field ρ_{SF} :

$$\rho_{SF} = -(T_{SF})_t^t + (T_{SF})_i^i = 2\left(\frac{2e^{2F_0}w(w - mW)}{N} - \mu^2\right)\phi^2. \quad (16)$$

IV. METHOD

A. Building the disk

To construct our models we take the following steps: First, we find the angular momentum l and the radius of the cusp r_{cusp} as the value at the minimum and the location of said minimum outside the event horizon of

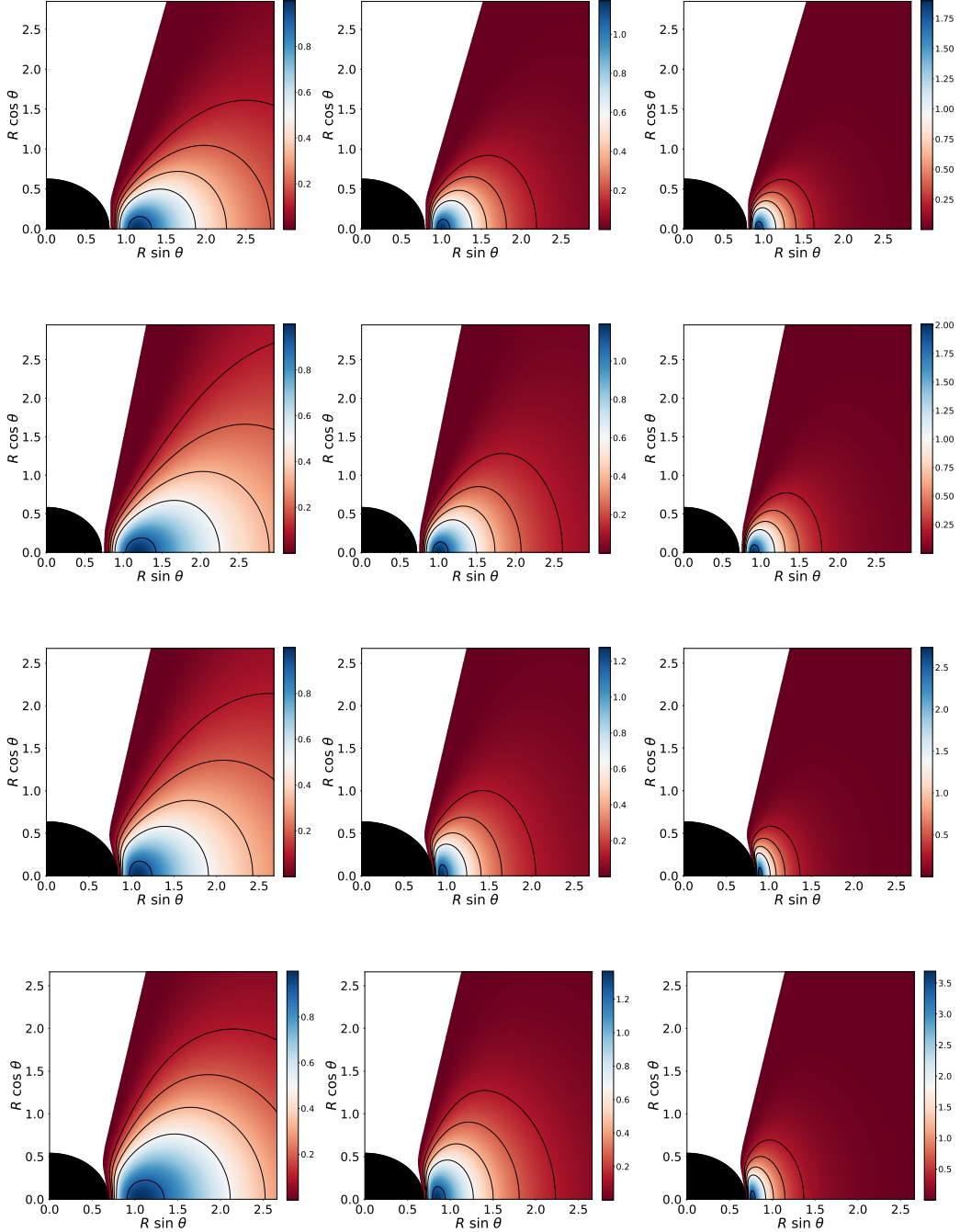


FIG. 3. Rest-mass density distribution using perimeteral coordinates. From top to bottom the rows correspond to the different models for the KBHsSH (I, II, III and IV). From left to right the columns correspond to different values of the magnetization parameter, namely non-magnetized ($\beta_{m_c} = 10^{10}$), mildly magnetized ($\beta_{m_c} = 1$) and strongly magnetized ($\beta_{m_c} = 10^{-10}$)

equation (6), this choice of angular momentum implies $r_{\text{cusp}} = r_{\text{mb}}$ and $l = l_K(r_{\text{mb}})$.

In this work, we use $q = \Gamma = 4/3$, the density at the disk centre $\rho_c = 1$ and the angular momentum distribution gives us $W_{\text{in}} = 0$. With this information we can compute all the relevant physical quantities.

B. Numerical method

V. RESULTS

As shown in [5] some SG: (compute which ones are embeddable and which are not) of our models are in the re-

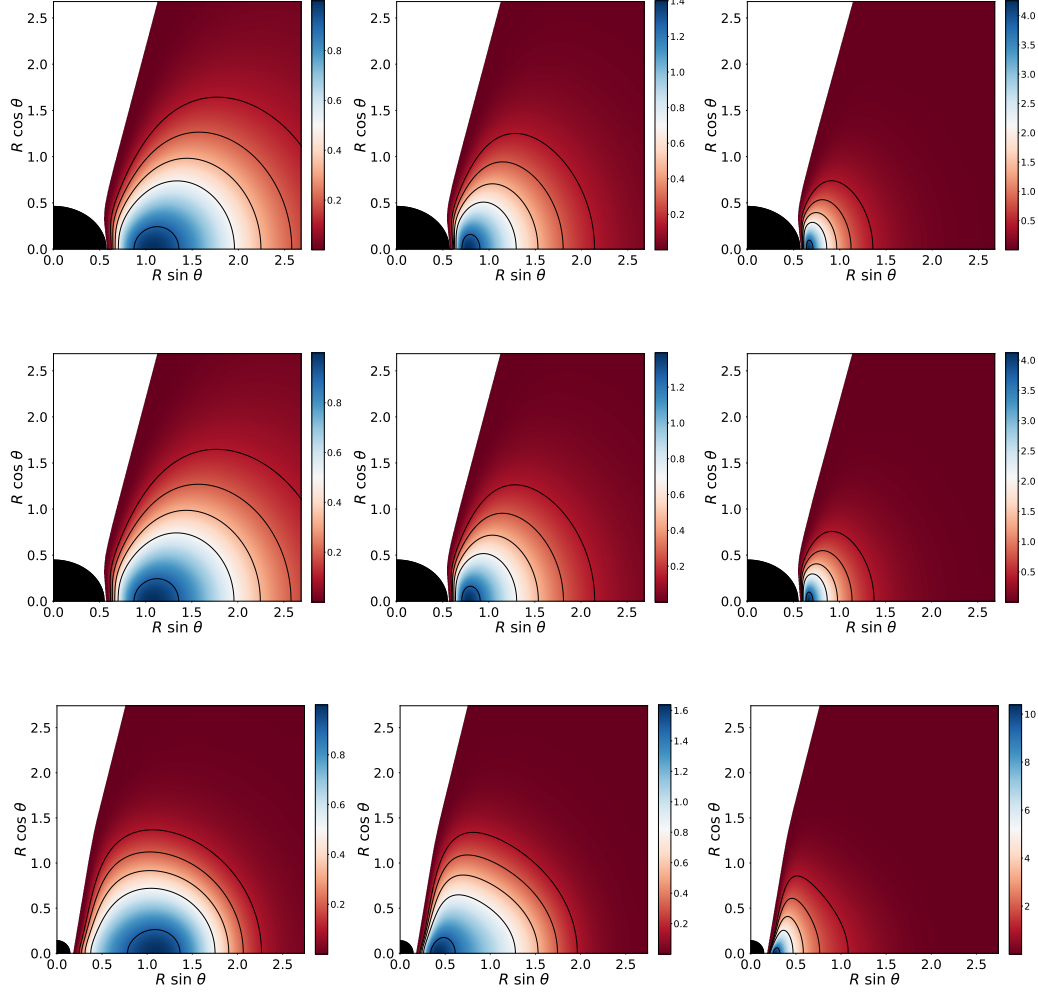


FIG. 4. Rest-mass density distribution using perimetal coordinates. From top to bottom the rows correspond to the different models for the KBHsSH (V, VI, VII). From left to right the columns correspond to different values of the magnetization parameter, namely non-magnetized ($\beta_{mc} = 10^{10}$), mildly magnetized ($\beta_{mc} = 1$) and strongly magnetized ($\beta_{mc} = 10^{-10}$)

gion of the domain of existence where the event horizon is not embeddable in \mathbb{E}^3 then, the shaded regions depicting the horizon that we show at several of the figures are not faithful representations of the horizon geometry. Nevertheless, we show them for the sake of clarity. Also, this led us to asking ourselves if this could also happen for the shape of the accretion tori and therefore, we should be conservative when extracting information about the morphology of the disks from the 2-dimensional plots. This

idea is discussed in appendixA.

VI. CONCLUSIONS

ACKNOWLEDGMENTS

-
- [1] C. A. R. Herdeiro and E. Radu, Physical Review Letters **112**, 221101 (2014), arXiv:1403.2757 [gr-qc].
 - [2] F. Daigne and J. A. Font, MNRAS **349**, 841 (2004), astro-ph/0311618.
 - [3] P. J. Montero, O. Zanotti, J. A. Font, and L. Rezzolla, MNRAS **378**, 1101 (2007), astro-ph/0702485.
 - [4] S. S. Komissarov, MNRAS **368**, 993 (2006), astro-ph/0601678.

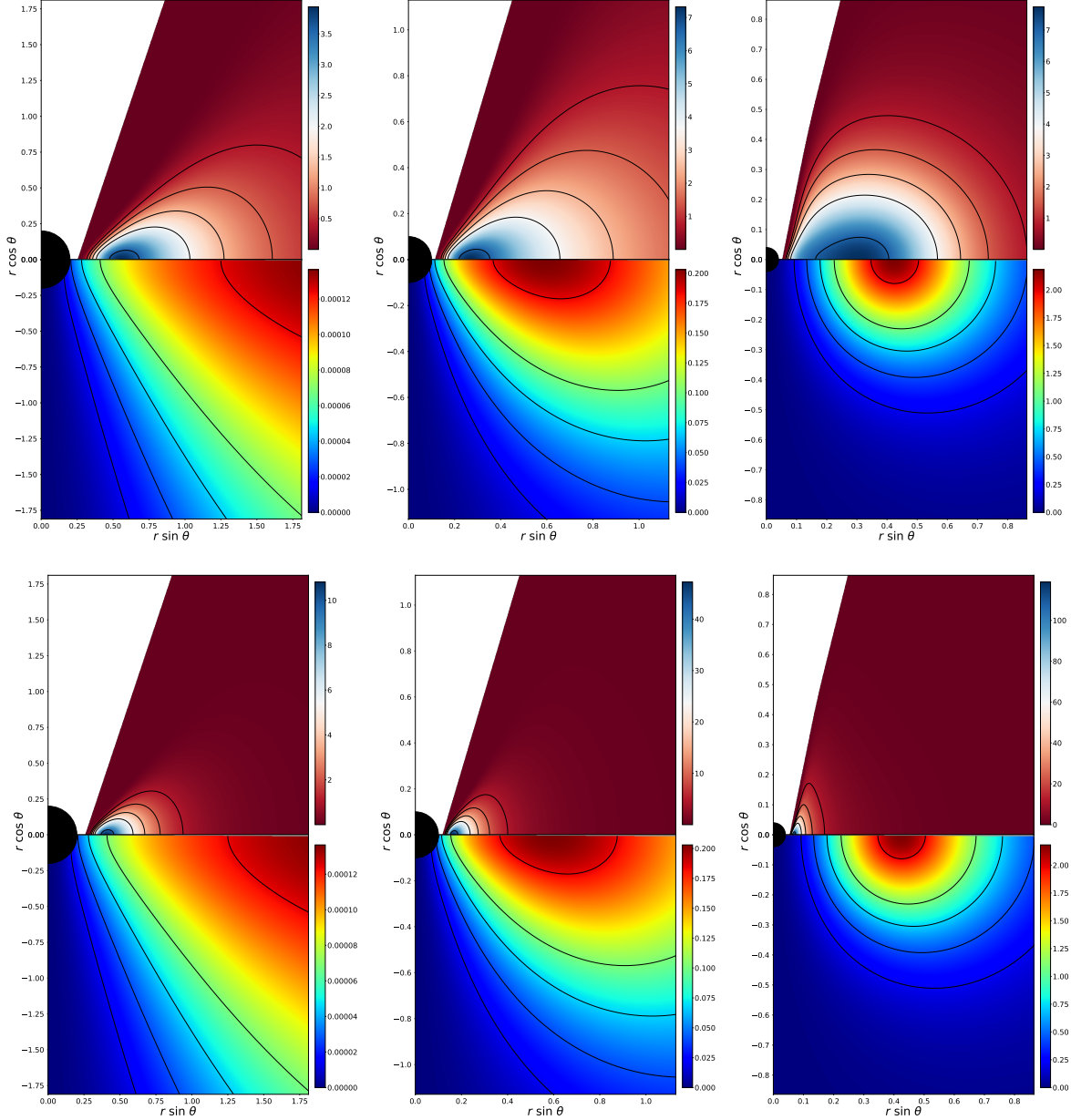


FIG. 5. Gravitational mass density ($-T_t^t + T_i^i$) distribution for the torus (up) and the scalar field (down). From left to right the columns correspond to different models (I, IV and VII). From top to bottom, the rows correspond to different values of the magnetization parameter, namely non-magnetized ($\beta_{mc} = 10^{10}$) and strongly magnetized ($\beta_{mc} = 10^{-10}$)

TABLE I. List of models of KBHsSH.

Model	M_{ADM}	J_{ADM}	M_H	J_H	M_{SF}	J_{SF}	r_H
I	0.415	0.172	0.393	0.15	0.022	0.022	0.2
II	0.630	0.403	0.340	0.121	0.063	0.282	0.221
III	0.797	0.573	0.365	0.172	0.573	0.432	0.111
IV	0.933	0.739	0.234	0.114	0.699	0.625	0.1
V	0.940	0.757	0.159	0.076	0.757	0.781	0.091
VI	0.959	0.795	0.087	0.034	0.872	0.781	0.088
VII	0.975	0.85	0.018	0.002	0.957	0.848	0.04

- [5] J. F. M. Delgado, C. A. R. Herdeiro, and E. Radu, ArXiv e-prints (2018), arXiv:1804.04910.
- [6] S. Gimeno-Soler and J. A. Font, Astron. Astrophys. **607**, A68 (2017), arXiv:1707.03867 [gr-qc].
- [7] M. Abramowicz, M. Jaroszynski, and M. Sikora, A&A **63**, 221 (1978).

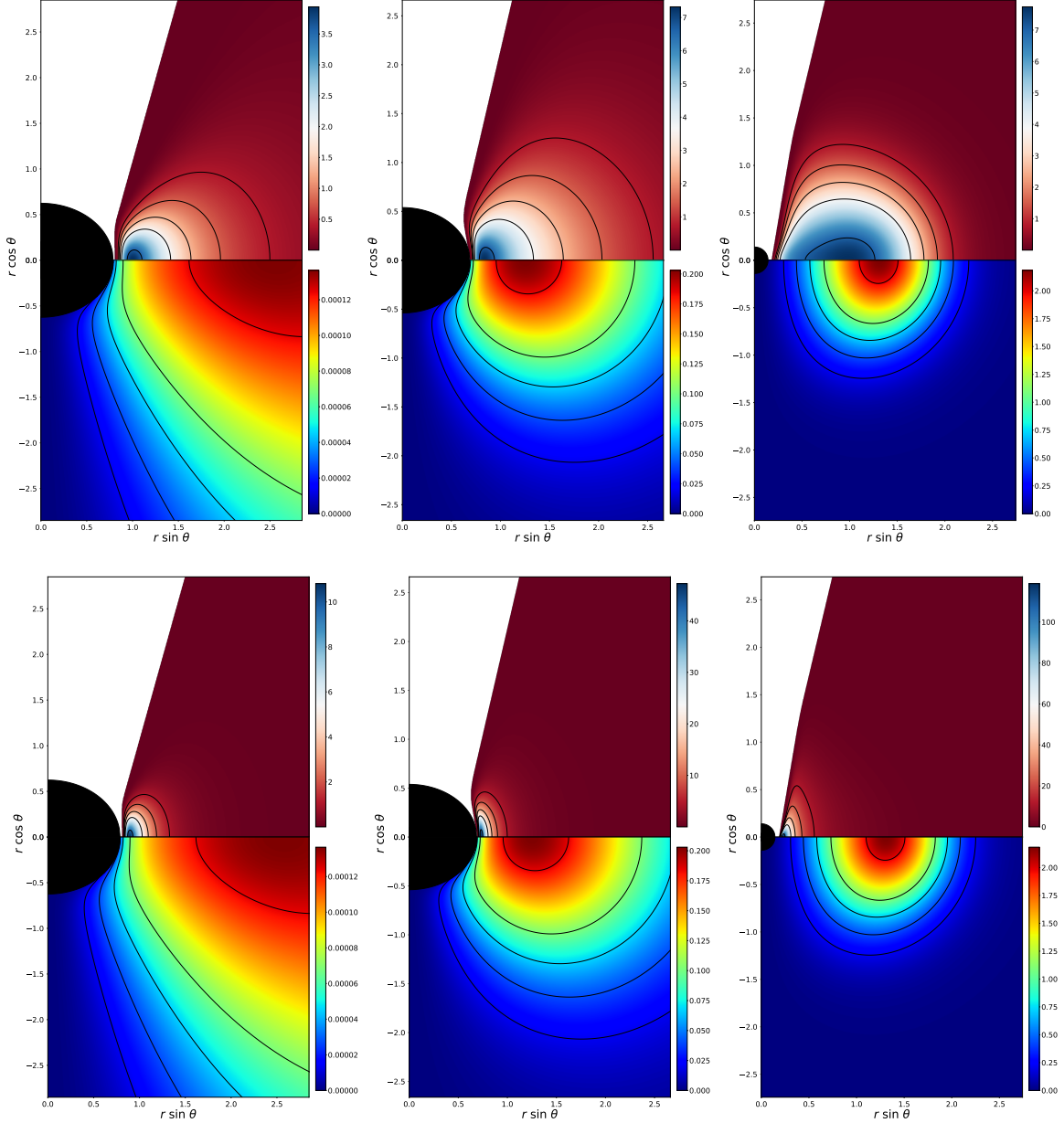


FIG. 6. Gravitational mass density ($-T_t^t + T_i^i$) distribution for the torus (up) and the scalar field (down) using perimetrical coordinates. From left to right the columns correspond to different models (I, IV and VII). From top to bottom, the rows correspond to different values of the magnetization parameter, namely non-magnetized ($\beta_{mc} = 10^{10}$) and strongly magnetized ($\beta_{mc} = 10^{-10}$)

Appendix A: Embedding of the accretion torus in \mathbb{E}^3

Following the same reasoning as in [5], we write the 2-metric for the surface of a torus as

$$d\sigma^2 = \frac{e^{2F_1}}{N} dr^2 + e^{2F_1} r^2 d\theta^2 + e^{2F_2} r^2 \sin^2 \theta d\phi^2, \quad (\text{A1})$$

and the condition $r = r(\theta)$ for the surface of the torus. The location of the surface of the torus $r(\theta)$ can be obtained integrating $r' = \frac{dr}{d\theta} = -\frac{\partial_\theta W}{\partial_r W}$ (equation (24) of [6]).

Using this, we can write equation (A1) as

$$d\sigma^2 = e^{2F_1} d\theta^2 \left(\frac{r'^2}{N} + r^2 \right) + e^{2F_2} r^2 \sin^2 \theta d\phi^2, \quad (\text{A2})$$

with the prime ' denoting partial differentiation with respect to θ . Then, we try the embedding in \mathbb{E}^3 with the Cartesian metric $d\sigma^2 = dX^2 + dY^2 + dZ^2$ and the embedding functions:

$$X + iY = f(\theta)e^{i\phi}, \quad Z = g(\theta), \quad (\text{A3})$$

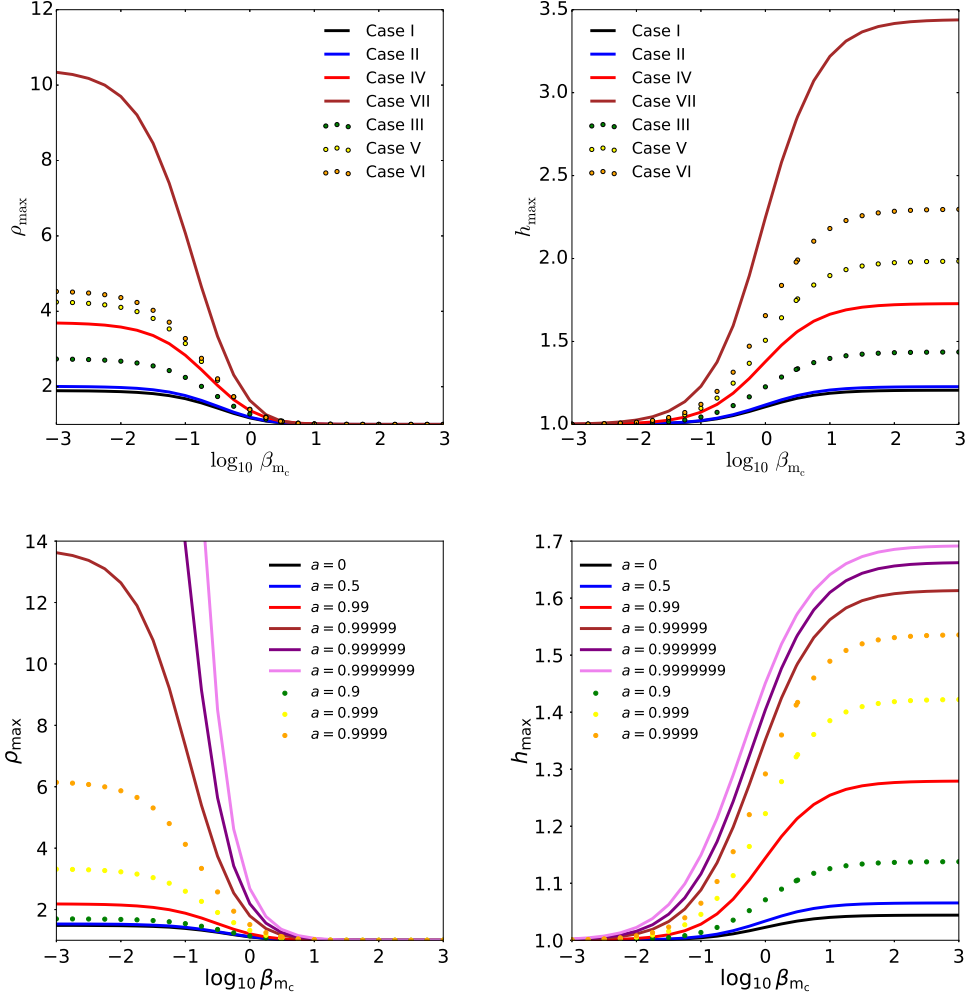


FIG. 7. Effects of the magnetization on the values for the maximum density (left) and enthalpy (right) of the disc. In the first row, we show this for all of our KBHsSH models. In the second row, we show this for a sequence of KBHs with increasing spin parameter.

then

$$f = e^{2F_2} r^2 \sin^2 \theta, \quad f'^2 + g'^2 = e^{2F_1} \left(\frac{r'^2}{N} + r^2 \right), \quad (\text{A4})$$

so we can write g'^2 as

$$g'^2 = e^{2F_1} \left(\frac{r'^2}{N} + r^2 \right) - e^{2F_2} (F'_2 r \sin \theta + r' \sin \theta + r \cos \theta)^2. \quad (\text{A5})$$

This result tells us that the r.h.s. of (A5) must be ≥ 0 in order for the embedding function to exist.

Appendix B: KBHsSH vs $h = 1$ approximation

In the figures ??, ??, ??, ??, ??, ?? we show the comparison between the results for KBHsSH using [3]

and [4]. The figures show good agreement for the highly magnetized case ($\beta_{mc} = 10^{-3}$) but not quite for the non-magnetized and mildly magnetized cases, especially for the model III. This is due to the $h = 1$ approximation breaking down. In the table ?? we show the correlation between the value of the potential at the centre and the specific enthalpy at the centre. It is easy to note that for higher absolute values of W_c we get values of h_c further away from the case $h = 1$. This is interesting because these high values of W_c (particularly the one for the model III) is unattainable for any KBH (as is shown by [7], the maximum value of W_c for a KBH is $W_c = 0.549$).

Appendix C: Finding l_{mb} and r_{mb}

Proof.

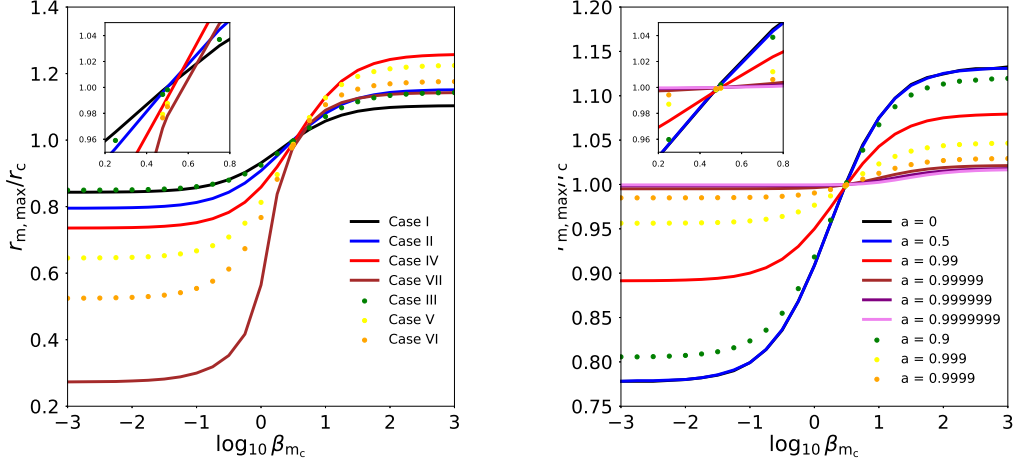


FIG. 8. Effects of the magnetization on the (perimeteral) location of the magnetic pressure maximum (divided by the the perimeteral radius of the centre) ($R_{\text{mag},\max}/R_c$). Left panel: KBHsSH models. Right panel: A sequence of KBHs with increasing spin parameter.

TABLE II. Disk parameters and values of their relevant physical magnitudes. For all the cases, we have $R_{\text{in}} = R_{\text{mb}}$ and $l = l_{\text{mb}}$

Model	l	W_c	R_{in}	R_c	β_{m_c}	h_{\max}	ρ_{\max}	p_{\max}	$p_{m,\max}$	R_{\max}	$R_{m,\max}$
I	0.934	-0.188	0.81	1.14	10^{10}	1.21	1.0	5.16×10^{-2}	5.50×10^{-12}	1.14	1.26
				1	1.10	1.17	3.11	10^{-2}	2.68×10^{-2}	1.01	1.06
				10^{-10}	1.0	1.90	1.10×10^{-11}	7.80×10^{-2}	0.93	0.96	
II	0.933	-0.205	0.75	1.18	10^{10}	1.23	1.0	5.69×10^{-2}	6.14×10^{-12}	1.18	1.36
				1	1.12	1.19	3.50×10^{-2}	2.97×10^{-2}	1.00	1.07	
				10^{-10}	1.0	2.01	1.30×10^{-11}	8.99×10^{-2}	0.91	0.94	
III	1.06	-0.362	0.84	1.07	10^{10}	1.44	1.0	0.109	1.21×10^{-11}	1.07	1.22
				1	1.23	1.28	7.22×10^{-2}	5.76×10^{-2}	0.95	0.99	
				10^{-10}	1.0	2.74	3.48×10^{-11}	0.206	0.89	0.91	
IV	1.16	-0.547	0.67	1.06	10^{10}	1.723	1.0	0.182	2.09×10^{-11}	1.06	1.34
				1	1.38	1.37	0.129	9.76×10^{-2}	0.85	0.91	
				10^{-10}	1.0	3.70	7.83×10^{-11}	0.408	0.76	0.78	
V	1.20	-0.685	0.58	1.07	10^{10}	1.98	1.0	0.246	2.76×10^{-11}	1.07	1.31
				1	1.51	1.40	0.178	0.132	0.78	0.87	
				10^{-10}	1.0	4.26	1.18×10^{-10}	0.579	0.67	0.69	
VI	1.20	-0.832	0.43	1.12	10^{10}	2.30	1.0	0.324	3.52×10^{-11}	1.12	1.32
				1	1.66	1.39	0.228	0.169	0.72	0.86	
				10^{-10}	1.0	4.54	1.57×10^{-10}	0.740	0.55	0.59	
VII	0.920	-1.236	0.18	1.10	10^{-10}	3.44	1.0	0.610	6.459×10^{-11}	1.10	1.25
				1	2.25	1.64	0.510	0.322	0.43	0.62	
				10^{-10}	1.0	10.42	7.03×10^{-10}	2.44	0.28	0.30	

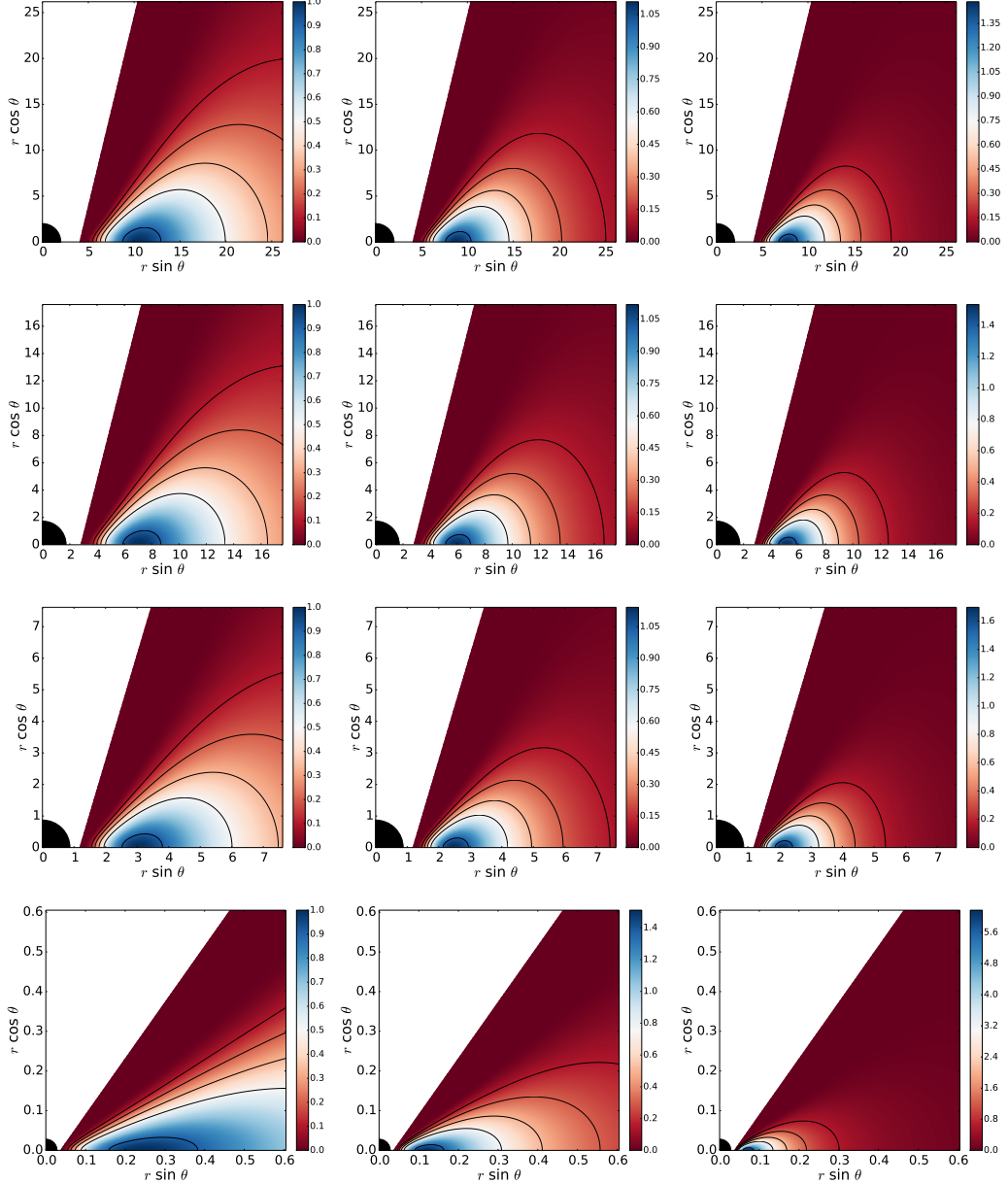


FIG. 9. Rest-mass density distribution. From top to bottom the rows correspond to a sequence of KBHs with increasing spin parameter a (0, 0.5, 0.9 and 0.9999). From left to right the columns correspond to different values of the magnetization parameter, namely non-magnetized ($\beta_{mc} = 10^{10}$), mildly magnetized ($\beta_{mc} = 1$) and strongly magnetized ($\beta_{mc} = 10^{-10}$)

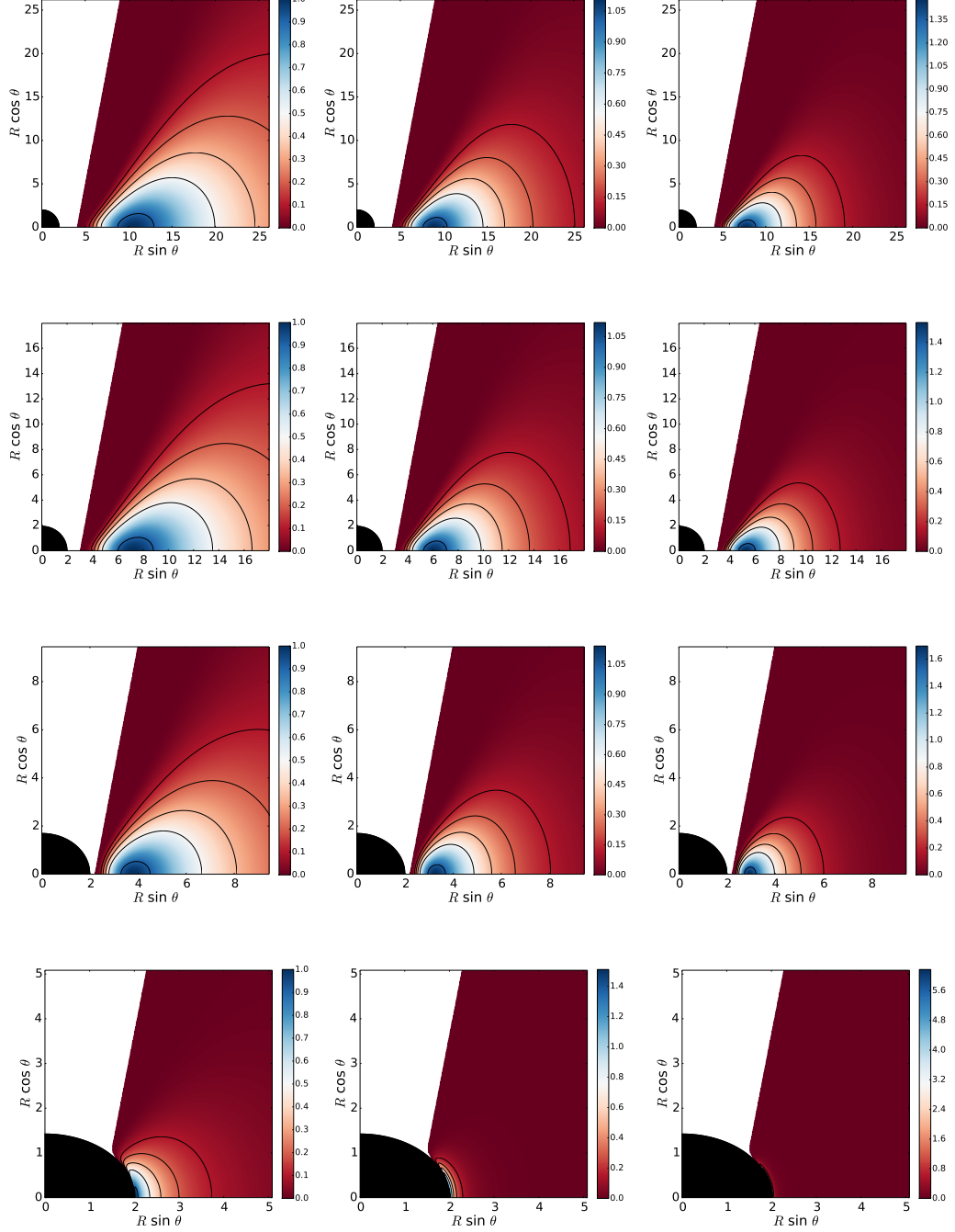


FIG. 10. Rest-mass density distribution using perimetric coordinates. From top to bottom the rows correspond to a sequence of KBHs with increasing spin parameter a (0, 0.5, 0.9 and 0.9999). From left to right the columns correspond to different values of the magnetization parameter, namely non-magnetized ($\beta_{mc} = 10^{10}$), mildly magnetized ($\beta_{mc} = 1$) and strongly magnetized ($\beta_{mc} = 10^{-10}$)

TABLE III. Disc parameters and values of their relevant physical magnitudes for the KBH case. For all the cases, we have $R_{\text{in}} = R_{\text{mb}}$ and $l = l_{\text{mb}}$

a	l	W_c	R_{in}	R_c	β_{m_c}	h_{max}	ρ_{max}	p_{max}	$p_{m,\text{max}}$	R_{max}	$R_{m,\text{max}}$	
0	4.00	-4.32×10^{-2}	4.00	10.47	10^{10}	1.04	1.0	1.10×10^{-2}	1.15×10^{-12}	10.47	11.86	
						1	1.02	1.11	6.29×10^{-3}	5.69×10^{-3}	8.81	9.52
						10^{-10}	1.0	1.48	1.83×10^{-12}	1.48×10^{-2}	7.70	8.14
0.5	3.41	-6.35×10^{-2}	2.99	7.12	10^{10}	1.07	1.0	1.64×10^{-2}	1.72×10^{-12}	7.19	8.14	
						1	1.03	1.12	9.43×10^{-3}	8.47×10^{-3}	6.05	6.53
						10^{-10}	1.0	1.53	2.81×10^{-12}	2.23×10^{-2}	5.29	5.59
0.9	2.63	-0.129	2.18	3.78	10^{10}	1.14	1.0	1.64×10^{-2}	3.65×10^{-12}	3.78	4.23	
						1	1.07	1.14	2.03×10^{-2}	1.78×10^{-2}	3.25	3.47
						10^{-10}	1.0	1.70	6.54×10^{-12}	4.92×10^{-2}	2.92	3.04
0.9999	2.02	-0.429	2.00015	2.034	10^{10}	1.54	1.0	0.134	1.61×10^{-11}	2.034	2.094	
						1	1.29	1.51	0.110	7.52×10^{-2}	2.0075	2.014
						10^{-10}	1.0	6.17	1.22×10^{-10}	0.491	2.0021	2.0030

TABLE IV. Values of the normalized spin parameter for the ADM quantities (a_{ADM}), for the BH horizon quantities (a_H), the horizon linear velocity (v_H) and the spin parameter corresponding to a KBH with a linear velocity equal to v_H , ($a_{H_{\text{eq}}}$).

Model	a_{ADM}	a_H	v_H	$a_{H_{\text{eq}}}$
I	0.9987	0.9712	0.7685	0.9663
II	1.014	0.3760	0.6802	0.9301
III	0.9032	1.295	0.7524	0.9608
IV	0.8489	2.082	0.5635	0.8554
V	0.8560	3.017	0.4438	0.7415
VI	0.9477	3.947	0.2988	0.5487
VII	0.8941	6.173	0.09732	0.1928

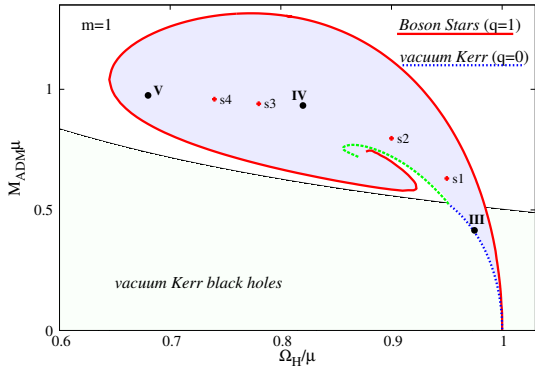


FIG. 11. Location of the models in the domain of existence of KBHsSH solutions. **update names.**